



LJMU Research Online

Verheul, J, Warmenhoven, J, Lisboa, P, Gregson, W, Vanrenterghem, J and Robinson, MA

Identifying generalised segmental acceleration patterns that contribute to ground reaction force features across different running tasks

<http://researchonline.ljmu.ac.uk/id/eprint/11063/>

Article

Citation (please note it is advisable to refer to the publisher's version if you intend to cite from this work)

Verheul, J, Warmenhoven, J, Lisboa, P, Gregson, W, Vanrenterghem, J and Robinson, MA (2019) Identifying generalised segmental acceleration patterns that contribute to ground reaction force features across different running tasks. Journal of Science and Medicine in Sport. ISSN 1878-1861

LJMU has developed [LJMU Research Online](http://researchonline.ljmu.ac.uk) for users to access the research output of the University more effectively. Copyright © and Moral Rights for the papers on this site are retained by the individual authors and/or other copyright owners. Users may download and/or print one copy of any article(s) in LJMU Research Online to facilitate their private study or for non-commercial research. You may not engage in further distribution of the material or use it for any profit-making activities or any commercial gain.

The version presented here may differ from the published version or from the version of the record. Please see the repository URL above for details on accessing the published version and note that access may require a subscription.

For more information please contact researchonline@ljmu.ac.uk

<http://researchonline.ljmu.ac.uk/>

1 **Identifying generalised segmental acceleration patterns that contribute to**
2 **ground reaction force features across different running tasks**

3

4 **Original research article**

5

6 **Authors:**

7 Jasper Verheul¹, John Warmenhoven^{2,3}, Paulo Lisboa⁴, Warren Gregson¹, Jos Vanrenterghem⁵, Mark
8 A. Robinson¹

9 1. Research Institute for Sport and Exercise Sciences, Liverpool John Moores University,
10 Liverpool, United Kingdom

11 2. Department of Exercise and Sports Science, The University of Sydney, Lidcombe, Australia

12 3. Performance People & Teams, Australian Institute of Sport, Canberra, Australia

13 4. Department of Applied Mathematics, Liverpool John Moores University, Liverpool, United
14 Kingdom

15 5. Department of Rehabilitation Sciences, KU Leuven, Leuven, Belgium

16

17 **Corresponding Author:**

18 Jasper Verheul (J.P.Verheul@ljmu.ac.uk)

19 Research Institute for Sport and Exercise Sciences, Liverpool John Moores University

20 Tom Reilly Building, Byrom Street, L3 5AF, Liverpool, United Kingdom

21

22 **Abstract word count:** 232

23 **Text-only word count:** 3041

24 **Number of figures and tables:** 2 figures and 1 table

25

26

27 **Abstract**

28 *Objective:* To support future developments of field-based biomechanical load monitoring tools, this
29 study aimed to identify generalised segmental acceleration patterns and their contribution to ground
30 reaction forces (GRFs) across different running tasks.

31 *Design:* Exploratory experimental design.

32 *Methods:* A multivariate principal component analysis (PCA) was applied to a combination of
33 segmental acceleration data from all body segments for fifteen team-sport athletes performing
34 accelerated, decelerated and constant low-, moderate- and high-speed running, and 90° cutting trials.
35 Segmental acceleration profiles were then reconstructed from each principal component (PC) and used
36 to calculate their specific GRF contributions.

37 *Results:* The first PC explained 48.57% of the acceleration variability for all body segments and was
38 primarily related to the between-task differences in the overall magnitude of the GRF impulse.
39 Magnitude and timing of high-frequency acceleration and GRF features (i.e. impact related
40 characteristics) were primarily explained by the second PC (12.43%) and also revealed important
41 between-task differences. The most important GRF characteristics were explained by the first five
42 PCs, while PCs beyond that primarily contained small contributions to the overall GRF impulse.

43 *Conclusions:* These findings show that a multivariate PCA approach can reveal generalised
44 acceleration patterns and specific segmental contributions to GRF features, but their relative
45 importance for different running activities are task dependent. Using segmental acceleration to assess
46 whole-body biomechanical loading generically across various movements may thus require task
47 identification algorithms and/or advanced sensor or data fusion approaches.

48 **Keywords:** Biomechanical loading; Principal component analysis; Segmental contributions; Running;
49 Accelerations

50

51 **Practical Implications**

- 52 • A multivariate PCA approach can be used to simultaneously identify general segmental
53 coordination patterns and specific segment contributions to GRF across running tasks, but
54 segment contributions to GRF vary between different movements.
- 55 • Caution should be practiced when using segmental acceleration signals to evaluate
56 biomechanical loads (e.g. from popular body-worn accelerometers), especially across different
57 tasks.
- 58 • Segmental acceleration information likely requires task identification algorithms and/or
59 advanced sensor or data fusion approaches to assess whole-body biomechanical loading
60 generically across various running movements.

61

62 **Introduction**

63 Although the physiological demands of sports have been monitored and investigated extensively in the
64 field, biomechanical loads are still poorly quantified and not well understood ¹. Ground reaction forces
65 (GRF) have, therefore, been suggested as a measure of external whole-body biomechanical loading,
66 which might be estimated from currently popular body-worn accelerometers ^{2,3}. Estimating GRF from
67 single accelerometers is, however, not straightforward ⁴⁻⁶. Whilst there might be the potential of using
68 full-body segmental accelerations to estimate GRF, reducing the number of segments to a number
69 more feasible in a practical setting has been shown to substantially increase the GRF error ^{2,7}. These
70 findings collectively suggest that estimating whole GRF waveforms accurately from segmental
71 accelerations across different tasks is unlikely to be feasible. Since human running comprises a
72 complex combination of simultaneous segmental movements however, more complex analyses may
73 identify fundamental movement features that contribute to the GRF and could still be captured with
74 accelerometers.

75 Principal component analysis (PCA) is a technique that can be used to reduce the amount of redundant
76 information and extract key characteristics (e.g. magnitude, difference and phase shift operators ^{13,20})
77 of highly-dimensional biomechanical data. For example, PCA has been used to analyse gait patterns ⁸⁻
78 ¹⁰ and postural control ^{11,12}, differentiate between pathological groups ^{10,13,14}, or quantify and evaluate
79 sports technique ¹⁵⁻¹⁷. Although applications of PCA in biomechanics have typically focussed on
80 waveform data for individual variables, multivariate PCA approaches allow for structures of
81 variability to be uncovered across multiple parameters at the same time ^{8,9,15}. Given the complexity of
82 segment coordination and interdependency of segmental accelerations during human running, a
83 simultaneous analysis of multiple acceleration profiles is desirable to examine if generalised
84 acceleration patterns across various segments exist and are related to specific GRF features. A
85 multivariate PCA approach in which different variables (e.g. segments, tasks, time) are combined,
86 might help to uncover such acceleration patterns and related GRF features across different running
87 tasks, and reveal which specific segmental accelerations together influence changes in GRF profiles.

88 It is unlikely that GRF can be predicted from one or several segmental accelerations using mechanical
89 methods ^{3,4,6}. However, these approaches typically use acceleration signals from predefined segments
90 deemed important for GRF but do not allow for an agnostic identification of generalised multi-
91 segmental contributions to the GRF. We hypothesised that if explicit GRF features are related to
92 generalised acceleration patterns across different running tasks, this could further inform the potential
93 for using segmental accelerations to assess whole-body biomechanical loads in running-based sports
94 (such as the choice of relevant segments or the feasibility to generalise across tasks). Therefore, this
95 study aimed to use a multivariate PCA approach to identify segmental acceleration patterns that
96 contribute to GRF features, to more comprehensively understand biomechanical loading and support
97 future developments of field-based biomechanical load monitoring tools.

98 **Methods**

99 *Data.* A previously described data set of full-body kinematics and GRF data for right foot
100 contacts of fifteen healthy team-sport athletes (12 males and 3 females, age 23±4 years, height 178±9
101 cm, body mass 73±10 kg, sports participation 7±5 h per week) were used for this study ². This study
102 was approved by the Liverpool John Moores University ethics committee and participants provided
103 written informed consent according to the ethics regulations.

104 Participants performed accelerated, decelerated, low- (2-3 m·s⁻¹) moderate- (4-5 m·s⁻¹) and high-speed
105 (>6 m·s⁻¹ including maximal sprinting) running, and 90° cutting ². Seventy-six marker trajectories
106 were measured from a three-dimensional motion capture system (Qualisys Inc., Gothenburg, Sweden),
107 while GRFs were measured from a force platform (Kistler Holding AG, Winterthur, Switzerland).
108 Kinematic and kinetic data were exported to Visual3D (C-motion, Germantown, MD, USA), which
109 was used to build a fifteen segment (head, trunk, pelvis, upper arms, forearms, hands, thighs, shanks
110 and feet) six-degree-of-freedom model ². Centre of mass (CoM) accelerations for each segment were
111 calculated as the double differentiation of segmental CoM positions.

112 *Normalisation and scaling.* All fifteen segmental CoM acceleration and GRF waveforms in
113 the mediolateral (x), anteroposterior (y) and vertical (z) direction during ground contact were
114 normalised to 101 data points for each trial. Segmental accelerations were then expressed as

115 acceleration vectors \mathbf{a} for every time point t (equation 1) (note: vectors and matrices will be referred to
 116 by using bold lowercase or capital letters respectively).

$$\mathbf{a}(t) = [ax_1(t), ay_1(t), az_1(t), ax_2(t), \dots, az_{15}(t)] \quad \text{Eq.1}$$

117 The combination of acceleration vectors for each trial thus formed a 101×45 acceleration matrix $\mathbf{A}^{\text{trial}}$.
 118 Trial-specific acceleration matrices were then combined in participant- and task-specific matrices
 119 $\mathbf{A}^{\text{part,task}}$ by vertically stacking each trial matrix $\mathbf{A}^{\text{trial}}$ per participant and task. These combined
 120 acceleration matrices $\mathbf{A}^{\text{part,task}}$ were normalised and scaled to 1) assure that every participant equally
 121 contributed to the variance of the total acceleration matrix, 2) reduce anthropometric differences
 122 between participants, 3) preserve relative segmental acceleration amplitudes and 4) correctly represent
 123 the portion of the total body mass of each segment¹². First, a participant- and task-specific mean
 124 acceleration vector $\overline{\mathbf{a}^{\text{part,task}}}$ was calculated and subtracted from each acceleration vector \mathbf{a} (equation
 125 2), to assure that the first PC described the direction of maximum variance in the segmental
 126 acceleration data.

$$\mathbf{A}^{\text{part,task}'}(t) = [(ax_1(t) - \overline{ax_1^{\text{part,task}}}), (ay_1(t) - \overline{ay_1^{\text{part,task}}}), \dots, (az_{15}(t) - \overline{az_{15}^{\text{part,task}}})] \quad \text{Eq.2}$$

127 Matrix $\mathbf{A}^{\text{subj,task}'}$ thus represented the acceleration deviations from the participant's mean segmental
 128 acceleration for each task. Secondly, acceleration vectors for each participant were divided by the
 129 mean Euclidean norm $\overline{\mathbf{euc}_{\text{norm}}^{\text{part,task}}}$ of all acceleration vectors (equation 3), to ensure that
 130 participants equally contributed to the variance of the total acceleration matrix and to minimise
 131 amplitude differences due to anthropometric differences^{11,18}.

$$\mathbf{A}^{\text{part,task}''}(t) = \frac{\mathbf{A}^{\text{part,task}'}(t)}{\overline{\mathbf{euc}_{\text{norm}}^{\text{part,task}}}} \quad \text{Eq.3}$$

132 Thirdly, each acceleration vector was normalised for the relative segmental masses to further account
 133 for anthropometric differences between segments. Acceleration vectors were multiplied by a weight
 134 vector \mathbf{w} (equation 4), which contained mass ratios of each segment relative to the total body mass¹⁹.

$$\mathbf{A}^{\text{part,task}'''}(t) = \mathbf{w} \cdot \mathbf{A}^{\text{part,task}''}(t) \quad \text{Eq.4}$$

135 Finally, the participant- and task-specific acceleration matrices for each participant $\mathbf{A}^{\text{part,task}''}$ were
 136 combined in one 48783×45 (15 participants · 6 tasks · number of trials per task (483 in total) · 101
 137 data points per trial) acceleration matrix \mathbf{A} .

138 *Principal component analysis.* A PCA was performed on the normalised and combined
 139 acceleration matrix \mathbf{A} . The results included 1) eigenvector matrix \mathbf{EV} consisting of 45 orthogonal
 140 eigenvectors \mathbf{ev}_k , (or ‘principal component vectors’) each indicating the largest acceleration variability
 141 for all segments, 2) eigenvalue matrix λ containing the eigenvalues λ_k which quantified the amount of
 142 variability described by each eigenvector \mathbf{ev}_k , with a strict decrease in the amount of variability with
 143 increasing k , and 3) time evolution coefficient matrix \mathbf{C} (or ‘score matrix’) describing how the original
 144 segmental acceleration data evolved along the new principal acceleration axes. \mathbf{C} was calculated by
 145 projecting each original normalised and scaled acceleration vector \mathbf{a} onto each PC_k of the eigenvector
 146 matrix ¹², according to equation 5.

$$\mathbf{c}_k(t) = \mathbf{a}(t) \cdot \mathbf{ev}_k \quad \text{Eq.5}$$

147 *Principal accelerations and principal GRF.* Participant- and task-specific principal
 148 acceleration (PA) matrices $\mathbf{PA}^{\text{part,task}}$ were reconstructed for each individual PC_k (equation 6) to
 149 investigate how patterns of acceleration contribute to the GRF, or the sum of the first k PCs (equation
 150 7) to examine the number of PCs required to adequately describe the whole GRF waveform. PCs were
 151 expressed in the original segmental acceleration space by decomposing reconstructed acceleration
 152 matrices into participant- and task-specific matrices, after which the normalisation and scaling steps
 153 were retraced.

$$\mathbf{PA}_k^{\text{part,task}}(t) = \overline{\mathbf{a}^{\text{part,task}}} + \overline{\mathbf{euc}_{\text{norm}}^{\text{part,task}}} \cdot \mathbf{w}^{-1} \cdot [\mathbf{C}_k \cdot \mathbf{ev}_k]^{\text{part,task}} \quad \text{Eq.6}$$

$$\mathbf{PA}_{1-k}^{\text{part,task}}(t) = \overline{\mathbf{a}^{\text{part,task}}} + \overline{\mathbf{euc}_{\text{norm}}^{\text{part,task}}} \cdot \mathbf{w}^{-1} \cdot \left[\sum_{k=1}^{1,2,\dots,45} \mathbf{C}_k \cdot \mathbf{ev}_k \right]^{\text{part,task}} \quad \text{Eq.7}$$

154 Since the reconstructed PAs are consistent with the laws of Newtonian mechanics, the principal
 155 segmental acceleration vectors \mathbf{pa} can be used to calculate principal GRF (PGRF) profiles. PGRF was

156 defined as the part of the overall GRF that is associated with the totality of all segment PAs combined.
 157 Resultant PGRF curves were calculated as the sum of the product of each segmental mass and
 158 principal CoM acceleration in the three directions, from each individual PC_k (equation 8), or from the
 159 sum of PAs reconstructed from the first k PCs (equation 9; Fig. 1).

$$\mathbf{PGRF}_k = \sqrt{\left(\sum_{n=1}^{15} (\mathbf{pa}_{k,n,x} \cdot m_n)\right)^2 + \left(\sum_{n=1}^{15} (\mathbf{pa}_{k,n,y} \cdot m_n)\right)^2 + \left(\sum_{n=1}^{15} (\mathbf{pa}_{k,n,z} \cdot m_n) + g \cdot \text{BM}\right)^2} \quad \text{Eq. 8}$$

$$\sum \mathbf{PGRF}_{1-k} = \sum_{pC=1}^k \left[\sqrt{\left(\sum_{n=1}^{15} (\mathbf{pa}_{k,n,x} \cdot m_n)\right)^2 + \left(\sum_{n=1}^{15} (\mathbf{pa}_{k,n,y} \cdot m_n)\right)^2 + \left(\sum_{n=1}^{15} (\mathbf{pa}_{k,n,z} \cdot m_n) + g \cdot \text{BM}\right)^2} \right] \quad \text{Eq. 9}$$

160 In which k is the PC number, **pa** the principal segmental acceleration in x, y or z direction, m the
 161 segmental mass, n the number of segments (n=15), g the gravitational acceleration (-9.81 m·s⁻¹) and
 162 BM the total body mass. Measured and calculated PGRF curves were normalised to each participant's
 163 body mass and accuracy evaluated as the curve root mean squared error (RMSE) relative to the
 164 measured GRF.

165 **Results**

166 Visual screening of PC results revealed that distinct acceleration and GRF features were primarily
 167 explained by the first five PCs, which explained 77.8% of all segmental acceleration variability across
 168 participants and tasks. Each additional PC (i.e. k>5) explained <3% variance of the original
 169 acceleration data and contributed <1% to the overall GRF. Therefore, only the first five PGRF and
 170 \sum PGRF profiles (see Fig. 1 for an example), and associated PAs were used for further qualitative
 171 analysis.

172 PC₁ explained 48.6% of the acceleration variability of all segments, which accounted for the majority
 173 of the overall GRF impulse (Fig. 2; Table 1). The largest amplitude of PA₁ occurred between ~10-70%
 174 of stance (Fig. A.1 and A.2) for decelerated and constant-speed running, but later during stance (~30-
 175 90%) for accelerated running. PA₁ magnitudes were typically the lowest for 90° cutting and running at
 176 slower speeds and the highest for the forearms and hands.

177 Including PC₂ reduced \sum PGRF errors by 25.5% across tasks (Table 1). PC₂ primarily explained high-
178 frequency acceleration contributions to the GRF impact peak associated with landing (Fig. 2), for all
179 tasks except accelerations, and were primarily expressed in PA₂ profiles of the right thigh, shank and
180 foot (stance leg segments) and pelvis. In contrast to the other tasks, PGRF₂ features for accelerated
181 running occurred during the second half of stance (i.e. ~50-90%).

182 Segmental accelerations from PC₃ were associated with two GRF features for constant-speed running,
183 but not for the other tasks. PGRF₃ contained small impact peak force components during early stance
184 (~20-30%), as well as a general contribution to GRF impulse during the second half of stance (Fig. 2).
185 Magnitudes for both GRF features increased with running speed and were primarily associated with
186 accelerations of leg and arm segments (Fig. A.2).

187 Compared to the first three PCs, PC₄ and PC₅ contained considerably less segmental acceleration
188 variability and distinct GRF features (Table 1). For accelerated running, these PCs made constant (but
189 small) GRF contributions from ~10-80% (PGRF₄) and ~0-50% (PGRF₅) of stance (Fig. 2), while for
190 other movements, PA₄ profiles were mainly associated with small GRF contributions during the first
191 ~40% of stance. For high-speed running, PGRF₅ contained a considerable amount of GRF impulse,
192 but not for the other tasks.

193 Including more PCs (i.e. $k > 5$) gradually increased the overall GRF and reduced \sum PGRF errors but
194 were not related to specific GRF features. To achieve \sum PGRF errors within 10% of the mean RMSE
195 for GRF from all 45 PCs (i.e. the original data), a total of 18 (accelerations), 2 (decelerations), 15 (90°
196 cuts), 7 (low-speed running), 4 (moderate-speed running) and 18 (high-speed running) PCs were
197 required, respectively.

198 **Discussion**

199 *Task-specific accelerations.* The aim of this study was to identify key contributions of
200 generalised acceleration patterns and specific segments to the GRF. The three primary modes of
201 variation described by PCA; a magnitude operator, difference operator and phase shift^{13,20}, were
202 evident in the first five PAs and PGRFs. First, segmental acceleration magnitude differences

203 associated with GRF impulse (i.e. overall loading of the body) and the impact peak were captured by
204 PC₁ and PC₂ respectively. Substantial amplitude variability in PA and PGRF profiles between tasks
205 showed that the magnitude of these GRF characteristics was strongly dependent on task (Fig. 2).
206 Secondly, PC₃ and PC₅ highlighted difference operator features. For accelerated running for example,
207 the main contributions of PGRF₃ and PGRF₅ to the overall GRF was during the first half of stance but
208 explained a much lower amount of force during push-off, while for constant-speed running this was
209 the other way around. Thirdly, clear phase shift characteristics were manifested in the first two PCs.
210 For example, the impulse peak (PGRF₁) and high-frequency acceleration and force features of PC₂
211 appeared in the first ~10-40% of stance for decelerations, constant-speed running and cutting tasks,
212 but much later during stance for accelerated running. These results show that PCA can identify general
213 acceleration patterns underlying specific GRF profiles, as well as highlight the relative importance of
214 these features for different running tasks.

215 PC₂ primarily contained acceleration and force features related to the GRF impact peak, for all tasks
216 except accelerations. These force peaks were mostly explained by high PA₂ peaks of the support leg's
217 foot, shank and thigh segment, and the pelvis to a lesser extent (Fig. A.1 and A.2). This supports
218 previous suggestions that the impact peak is primarily associated with stance leg accelerations²¹⁻²³.
219 Moreover, despite the absence of visual impact peaks in GRF waveforms for non-rearfoot running
220 gaits (e.g. sprinting), force frequencies associated with these initial force peaks are still present^{24,25}.
221 Clear impact force peaks were indeed found in PGRF₂ profiles for high-speed running, for which
222 runners typically switched to a forefoot landing technique (Fig. 2). The present PCA approach thus
223 further supports the presence of impact force peaks in non-rearfoot running, despite their visual
224 absence in the GRF waveform.

225 For accelerated running, PA₂ profiles of the support leg's foot, shank and thigh segments were mainly
226 related to a force peak during the second half of stance (Fig. 2). In addition, the smoother impacts of
227 landing during accelerations were better explained by PC₅ and thus less important for the overall
228 biomechanical load on the body. This highlights the importance of force production when pushing off
229 the ground in acceleration movements, compared to other tasks in which braking (force) is emphasised

230 more. Using PCA across multiple tasks can thus not only identify generic acceleration patterns, but
231 also explain their relative importance for different running movements.

232 The results of this study highlight that segment contributions to GRF are movement dependent. These
233 findings could explain why generalised methods to predict GRF from one or a few acceleration signals
234 cannot lead to accurate GRF estimates across different tasks ^{2,7}. For example, a specific segment (or
235 combination of segments) might be suitable to estimate GRF profiles for sprinting, while the same
236 segments are not so suitable to describe the GRF for decelerated running. Therefore, one should be
237 cautious when using generic biomechanical models or approaches to estimate GRF and/or assess
238 external biomechanical loads from segmental accelerations across different running tasks.

239 *Segment-specific accelerations.* Trunk accelerometry is arguably the most commonly used
240 acceleration signal for assessing biomechanical loads in different sports ²⁶⁻²⁸. Although the trunk is
241 thought to be the main contributor to GRF ²¹, trunk PA₁ profiles were very similar to other segments,
242 for all tasks (Fig. A.1 and A.2). Moreover, higher PCs (i.e. $k > 1$) did not explain any considerable
243 additional trunk acceleration features. These findings thus suggest that the trunk's large contributions
244 to GRF are primarily due to its large mass rather than the characteristics of its acceleration. The value
245 of using trunk accelerometry alone for biomechanical load monitoring purposes is thus probably
246 limited.

247 PAs of the forearm and hand segments typically had a high magnitude of acceleration (Fig. A.1 and
248 A.2) but did not make any distinct contribution to the specific GRF features in the first five PCs.
249 Furthermore, for decelerated and low- to moderate-speed running considerably less PCs were required
250 to achieve \sum PGRF errors within 10% of the mean RMSEs from all 45 PCs. This is possibly caused by
251 the more profound and complex arm movements (explained by PCs beyond the first five) during
252 acceleration, cutting and sprinting movements. Therefore, although arm movements (but also swing
253 leg motion) are not the primary contributors to GRF, these segments do account for a considerable part
254 of overall GRF impulse. These findings highlight that all segments should be considered when
255 assessing whole-body loading, especially for sports in which dynamic and high-intensity tasks are
256 frequently performed.

257 It should be acknowledged that directly measuring PAs (e.g. from multiple body-worn accelerometers)
258 may not be feasible in training and competition environments, making it difficult to translate the
259 present findings to a field-based load monitoring context. The multivariate PCA approach used in this
260 study could, however, uncover a deeper layer of complexity and highlight key characteristics in a
261 high-dimensional acceleration data set. This complexity adds to previous findings that reconstructing
262 GRF waveforms from less than all segments across different tasks is unlikely feasible ². The PCA
263 allowed for different acceleration combinations and key features to be detected, which provides
264 practical insight for what sensors to include when using too many sensors is an issue in the field.
265 Regardless, the complexity of segmental contributions to GRF outlined in this study further
266 emphasises that estimating biomechanical loading from accelerations is not straightforward, especially
267 across different tasks. Therefore, using body-worn accelerometry to estimate whole-body
268 biomechanical loading across various movements likely requires task identification algorithms and/or
269 advanced sensor or data fusion approaches (e.g.²⁹).

270 *Limitations.* The methods described in this study have several limitations. First, PCA was
271 deliberately performed on the combined segmental accelerations for multiple participants and tasks.
272 The results are thus a general representation of how segmental acceleration contribute to GRF, across
273 different running tasks. Unique loading or movement features for individual athletes or tasks may thus
274 not be highlighted and future research could consider task- and/or participant-specific PCA. Secondly,
275 using resultant accelerations and GRFs did not allow for identifying direction-specific acceleration and
276 GRF features. However, this study aimed to evaluate generic acceleration patterns related to overall
277 biomechanical load features. Moreover, body-worn accelerometers cannot typically distinguish
278 between global x-y-z directions and using resultant accelerations was deemed more feasible for
279 potential translations of our findings to a field-based load monitoring context. Thirdly, segmental
280 acceleration data were normalised by a weighting vector based on a standardised mass distribution ¹⁹.
281 Due to typical anthropometric differences between participants, defining and applying an
282 individualised mass distribution could affect the results. Although this was beyond the scope of this
283 study, future work could consider if personalised normalisation may be beneficial.

284 **Conclusions**

285 This study aimed to identify general segmental acceleration patterns associated with GRF features that
286 might be used to assess whole-body biomechanical loads. Although a multivariate PCA could reveal
287 generic acceleration patterns and specific segmental contributions to GRF, the relative importance of
288 these features varied between tasks. Using segmental acceleration to assess whole-body biomechanical
289 loading generically across different movements thus likely requires task identification algorithms
290 and/or advanced sensor or data fusion approaches.

291 **Acknowledgements**

292 This study did not receive any external financial support.

293 **Supplementary files**

294 Fig. A.1 and A.2 can be found in Appendix A, which is available as an online supplementary
295 document.

296 **References**

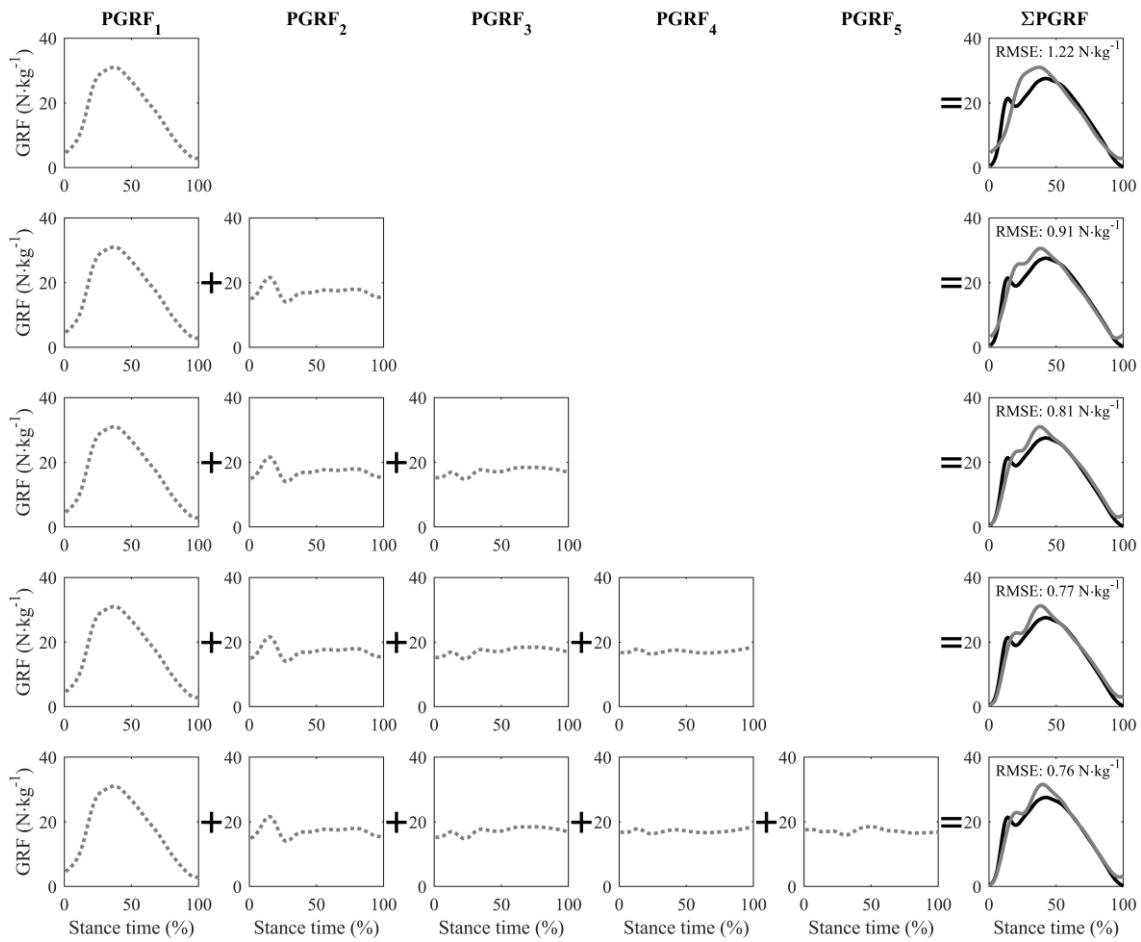
- 297 1. Vanrenterghem J, Nedergaard NJ, Robinson MA, Drust B. Training Load Monitoring in Team
298 Sports: A Novel Framework Separating Physiological and Biomechanical Load-Adaptation
299 Pathways. *Sport Med.* 2017;47(11):2135-2142. doi:10.1007/s40279-017-0714-2
- 300 2. Verheul J, Gregson W, Lisboa PJ, Vanrenterghem J, Robinson MA. Whole-body
301 biomechanical load in running-based sports: The validity of estimating ground reaction forces
302 from segmental accelerations. *J Sci Med Sport.* 2019;22(6):716-722.
303 doi:10.1016/j.jsams.2018.12.007
- 304 3. Nedergaard NJ, Robinson MA, Eusterwiemann E, Drust B, Lisboa PJ, Vanrenterghem J. The
305 Relationship Between Whole-Body External Loading and Body-Worn Accelerometry During
306 Team-Sport Movements. *Int J Sports Physiol Perform.* 2017;12(1):18-26.
307 [https://search.ebscohost.com/login.aspx?direct=true&db=sph&AN=121191349&site=ehost-](https://search.ebscohost.com/login.aspx?direct=true&db=sph&AN=121191349&site=ehost-live)
308 [live.](https://search.ebscohost.com/login.aspx?direct=true&db=sph&AN=121191349&site=ehost-live)
- 309 4. Nedergaard NJ, Verheul J, Drust B, et al. The feasibility of predicting ground reaction forces
310 during running from a trunk accelerometry driven mass-spring-damper model. *PeerJ.*
311 2018;6:e6105. doi:10.7717/peerj.6105
- 312 5. Raper DP, Witchalls J, Philips EJ, Knight E, Drew MK, Waddington G. Use of a tibial
313 accelerometer to measure ground reaction force in running: A reliability and validity
314 comparison with force plates. *J Sci Med Sport.* 2018;21(1):84-88.
315 doi:10.1016/j.jsams.2017.06.010
- 316 6. Edwards S, White S, Humphreys S, Robergs R, O'Dwyer N. Caution using data from triaxial
317 accelerometers housed in player tracking units during running. *J Sports Sci.* 2018:1-9.
318 doi:10.1080/02640414.2018.1527675
- 319 7. Pavei G, Seminati E, Cazzola D, Minetti AE. On the estimation accuracy of the 3D body center

- 320 of mass trajectory during human locomotion: Inverse vs. forward dynamics. *Front Physiol.*
321 2017;8(129):1-13. doi:10.3389/fphys.2017.00129
- 322 8. Daffertshofer A, Lamoth CJCC, Meijer OG, Beek PJ. PCA in studying coordination and
323 variability: A tutorial. *Clin Biomech.* 2004;19(4):415-428.
324 doi:10.1016/j.clinbiomech.2004.01.005
- 325 9. Troje NF. Decomposing biological motion: A framework for analysis and synthesis of human
326 gait patterns. *J Vis.* 2002;2:371-387. <http://journalofvision.org/2/5/2/>.
- 327 10. Federolf PA, Boyer KA, Andriacchi TP. Application of principal component analysis in
328 clinical gait research: Identification of systematic differences between healthy and medial
329 knee-osteoarthritic gait. *J Biomech.* 2013;46(13):2173-2178.
330 doi:10.1016/j.jbiomech.2013.06.032
- 331 11. Federolf PA, Roos L, Nigg BM. Analysis of the multi-segmental postural movement strategies
332 utilized in bipedal, tandem and one-leg stance as quantified by a principal component
333 decomposition of marker coordinates. *J Biomech.* 2013;46:2626-2633.
334 doi:10.1016/j.jbiomech.2013.08.008
- 335 12. Federolf PA. A novel approach to study human posture control: "Principal movements"
336 obtained from a principal component analysis of kinematic marker data. *J Biomech.*
337 2016;49:364-370. doi:10.1016/j.jbiomech.2015.12.030
- 338 13. Wrigley AT, Albert WJ, Deluzio KJ, Stevenson JM. Differentiating lifting technique between
339 those who develop low back pain and those who do not. *Clin Biomech.* 2005;20:254-263.
340 doi:10.1016/j.clinbiomech.2004.11.008
- 341 14. Deluzio KJ, Wyss UP, Zee B, Costigan PA, Sorbie C. Principal component models of knee
342 kinematics and kinetics: Normal vs. pathological gait patterns. *Hum Mov Sci.* 1997;16:201-217.
343 doi:10.1016/S0167-9457(96)00051-6

- 344 15. Federolf PA, Reid R, Gilgien M, Haugen P, Smith G. The application of principal component
345 analysis to quantify technique in sports. *Scand J Med Sci Sports*. 2014;24:491-499.
346 doi:10.1111/j.1600-0838.2012.01455.x
- 347 16. Boyer KA, Silvernail JF, Hamill J. The Role of Running Mileage on Coordination Patterns in
348 Running. *J Appl Biomech*. 2014;30:649-654. doi:10.1123/JAB.2013-0261
- 349 17. Warmenhoven J, Cobley S, Draper C, Harrison A, Bargary N, Smith R. How gender and boat-
350 side affect shape characteristics of force – angle profiles in single sculling: Insights from
351 functional data analysis. *J Sci Med Sport*. 2018;21(5):533-537.
352 doi:10.1016/j.jsams.2017.08.010
- 353 18. Gløersen Ø, Myklebust H, Hallén J, Federolf PA. Technique analysis in elite athletes using
354 principal component analysis. *J Sports Sci*. 2018;36(2):229-237.
355 doi:10.1080/02640414.2017.1298826
- 356 19. Dempster WT. Space requirements of the seated operator: Geometrical, Kinematic, and
357 Mechanical Aspects of the Body With Special Reference to the Limbs. *WADC Tech Rep*.
358 1955:55-159.
- 359 20. Brandon SCE, Graham RB, Almosnino S, Sadler EM, Stevenson JM, Deluzio KJ. Interpreting
360 principal components in biomechanics: Representative extremes and single component
361 reconstruction. *J Electromyogr Kinesiol*. 2013;23:1304-1310.
362 doi:10.1016/j.jelekin.2013.09.010
- 363 21. Bobbert MF, Schamhardt HC, Nigg BM. Calculation of vertical ground reaction force
364 estimates during running from positional data. *J Biomech*. 1991;24(12):1095-1105.
365 doi:10.1016/0021-9290(91)90002-5
- 366 22. Shorten M, Mientjes MIV. The “heel impact” force peak during running is neither “heel” nor
367 “impact” and does not quantify shoe cushioning effects. *Footwear Sci*. 2011;3(1):41-58.

- 368 doi:10.1080/19424280.2010.542186
- 369 23. Clark KP, Ryan LJ, Weyand PG. A general relationship links gait mechanics and running
370 ground reaction forces. *J Exp Biol.* 2017;220(2):247-258. doi:10.1242/jeb.138057
- 371 24. Hamill J, Gruber AH. Is changing footstrike pattern beneficial to runners? *J Sport Heal Sci.*
372 2017;6:146-153. doi:10.1016/j.jshs.2017.02.004
- 373 25. Gruber AH, Edwards WB, Hamill J, Derrick TR, Boyer KA. A comparison of the ground
374 reaction force frequency content during rearfoot and non-rearfoot running patterns. *Gait*
375 *Posture.* 2017. doi:10.1016/j.gaitpost.2017.04.037
- 376 26. Colby MJ, Dawson B, Heasman J, Rogalski B, Gabbett TJ. Accelerometer and GPS-Derived
377 Running Loads and Injury Risk in Elite Australian Footballers. *J Strength Cond Res.*
378 2014;28(8):2244-2252.
- 379 27. Akenhead R, Marques JB, Paul DJ. Accelerometer load: a new way to measure fatigue during
380 repeated sprint training? *Sci Med Footb.* 2017;1(2):151-156.
381 doi:10.1080/24733938.2017.1330550
- 382 28. Buchheit M, Gray A, Morin J-B. Assessing stride variables and vertical stiffness with GPS-
383 embedded accelerometers: preliminary insights for the monitoring of neuromuscular fatigue on
384 the field. *J Sport Sci Med.* 2015;(14):698-701.
- 385 29. Johnson WR, Mian A, Robinson MA, Verheul J, Lloyd DG, Alderson JA. Multidimensional
386 ground reaction forces and moments from wearable sensor accelerations via deep learning.
387 *arXiv Prepr.* 2019.
- 388

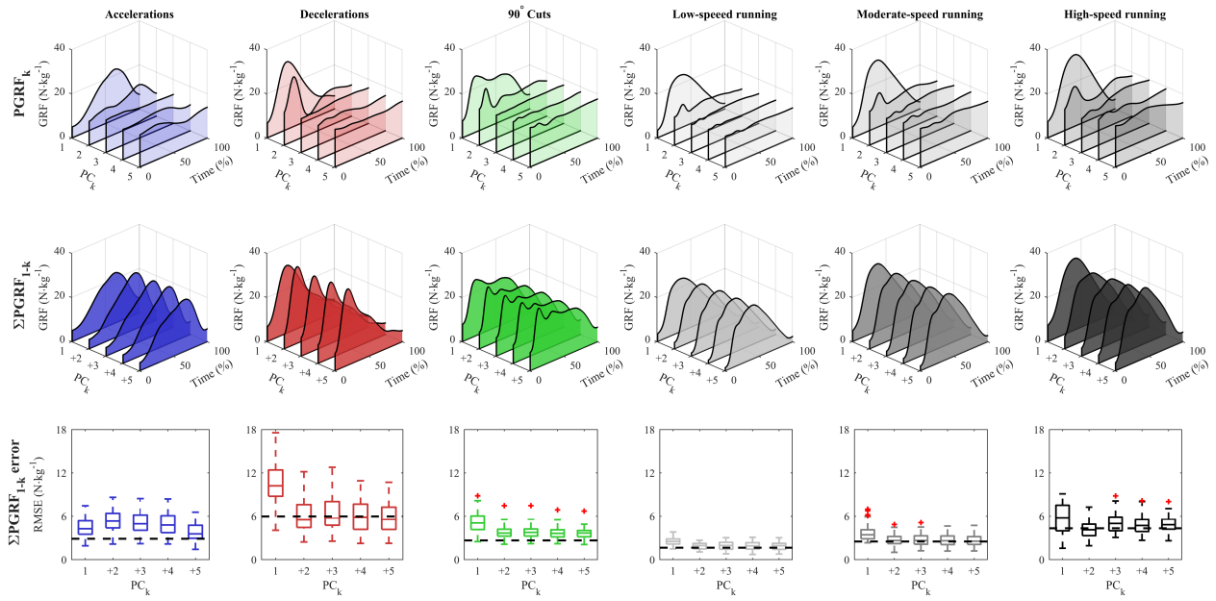
389 **Figures and tables**



390

391 **Figure 1** Representative example of individual and summed ground reaction force (GRF) profiles
 392 reconstructed from the first five principal components (PCs), for a single trial of running at a constant
 393 moderate speed. Individual principal GRFs (PGRFs; grey dotted lines) were added together as the
 394 summed PGRFs (Σ PGRFs; grey solid lines) for the first k PCs and compared to the measured GRF
 395 (black solid line) by the curve root mean square error (RMSE).

396



397

398 **Figure 2** Mean principal ground reaction forces (PGRFs) calculated from the first five principal
 399 components (PCs), for each task. PGRFs were calculated from principal accelerations (PAs)
 400 reconstructed from either the k^{th} PC (top row), or the sum of the first k PCs (ΣPGRF_{1-k} ; middle row).
 401 Root mean square errors (RMSE; bottom row) are mean errors for the ΣPGRF profiles and
 402 horizontal black line represents the RMSE for ΣPGRFs from all 45 PCs (i.e. the original data).

Table 1 Principal components and ground reaction forces for the different tasks

	Principal components (k)					
	1	2	3	4	5	45
λ_k (%)	48.57	12.43	8.56	4.44	3.78	0
Cumulative λ (%)	48.57	60.99	69.55	73.99	77.77	100
	Σ PGRF RMSE (N·kg ⁻¹)					
Accelerations (n=80)	4.46 ±1.3	5.37 ±1.5	5.09 ±1.5	4.93 ±1.5	3.88 ±1.2	2.89 ±0.7
Decelerations (n=83)	10.69 ±3.1	6.18 ±2.3	6.44 ±2.4	6.11 ±2.2	5.88 ±2	5.97 ±1.8
90° Cuts (n=88)	5.11 ±1.3	3.77 ±0.9	3.79 ±0.9	3.65 ±0.8	3.61 ±0.7	2.66 ±0.7
Constant speed running						
Low (2-3 m·s ⁻¹ ; n=81)	2.53 ±0.5	1.89 ±0.4	1.93 ±0.5	1.92 ±0.5	1.87 ±0.5	1.65 ±0.4
Moderate (4-5 m·s ⁻¹ ; n=80)	3.74 ±1.1	2.70 ±0.8	2.82 ±0.9	2.72 ±0.8	2.66 ±0.7	2.51 ±0.6
High (>6 m·s ⁻¹ ; n=71)	5.67 ±2	4.14 ±1.2	5.03 ±1.2	4.71 ±1.2	4.84 ±1.1	4.34 ±1.3
All tasks (n=483)	5.38 ±3.1	4.01 ±2	4.17 ±2.1	4.00 ±1.9	3.78 ±1.8	3.33 ±1.8

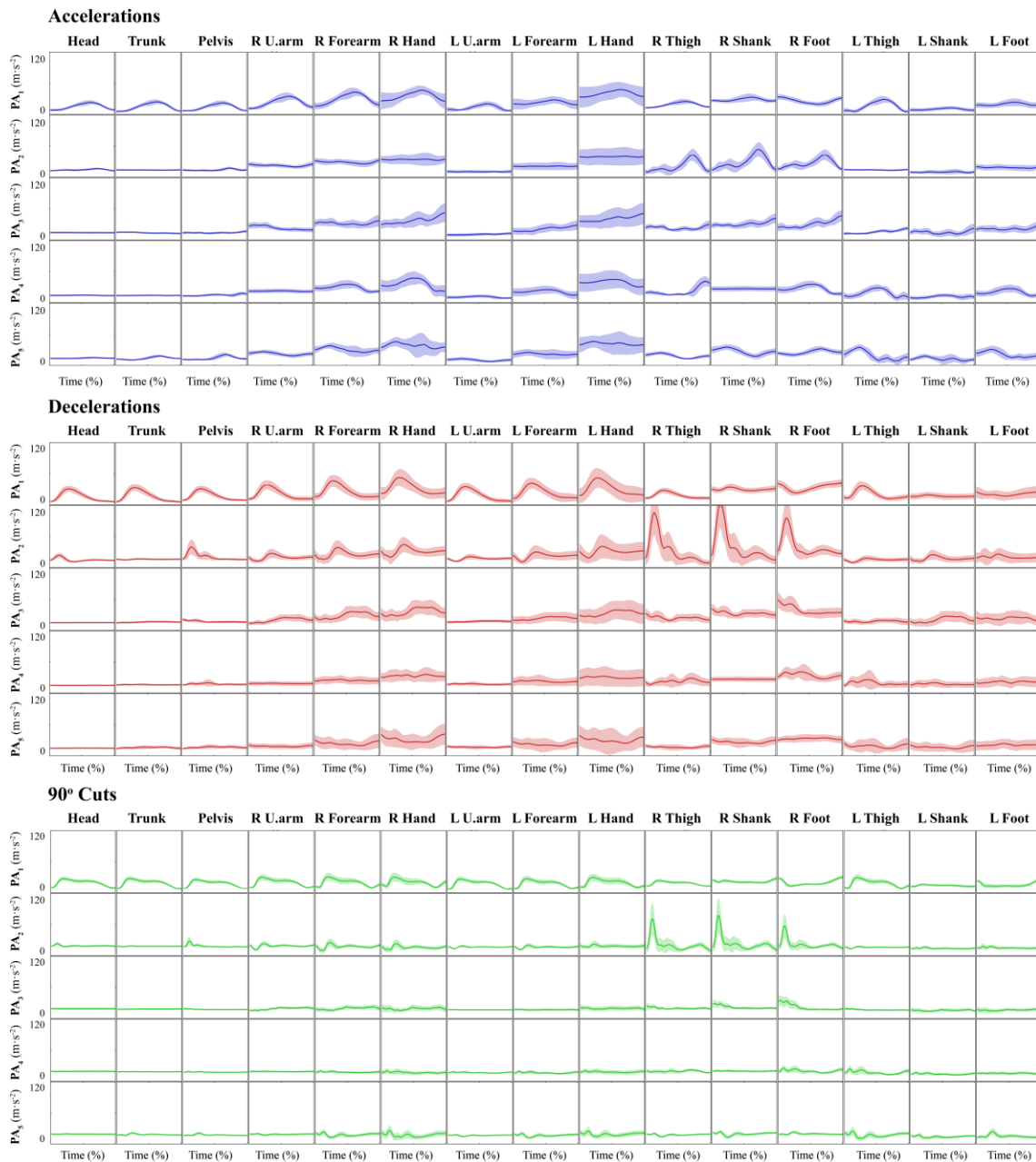
Summed principal ground reaction force (Σ PGRF) error results from the first k principal components (PCs), as well as all 45 PCs (i.e. original data). Eigenvalues λ_k represent the normalised amount of segmental acceleration variance explained by each PC_k. Root mean square errors (RMSE) are mean \pm standard deviation values per PC_k for each task.

403

404

405 **Appendix A: Principal segmental accelerations**

406

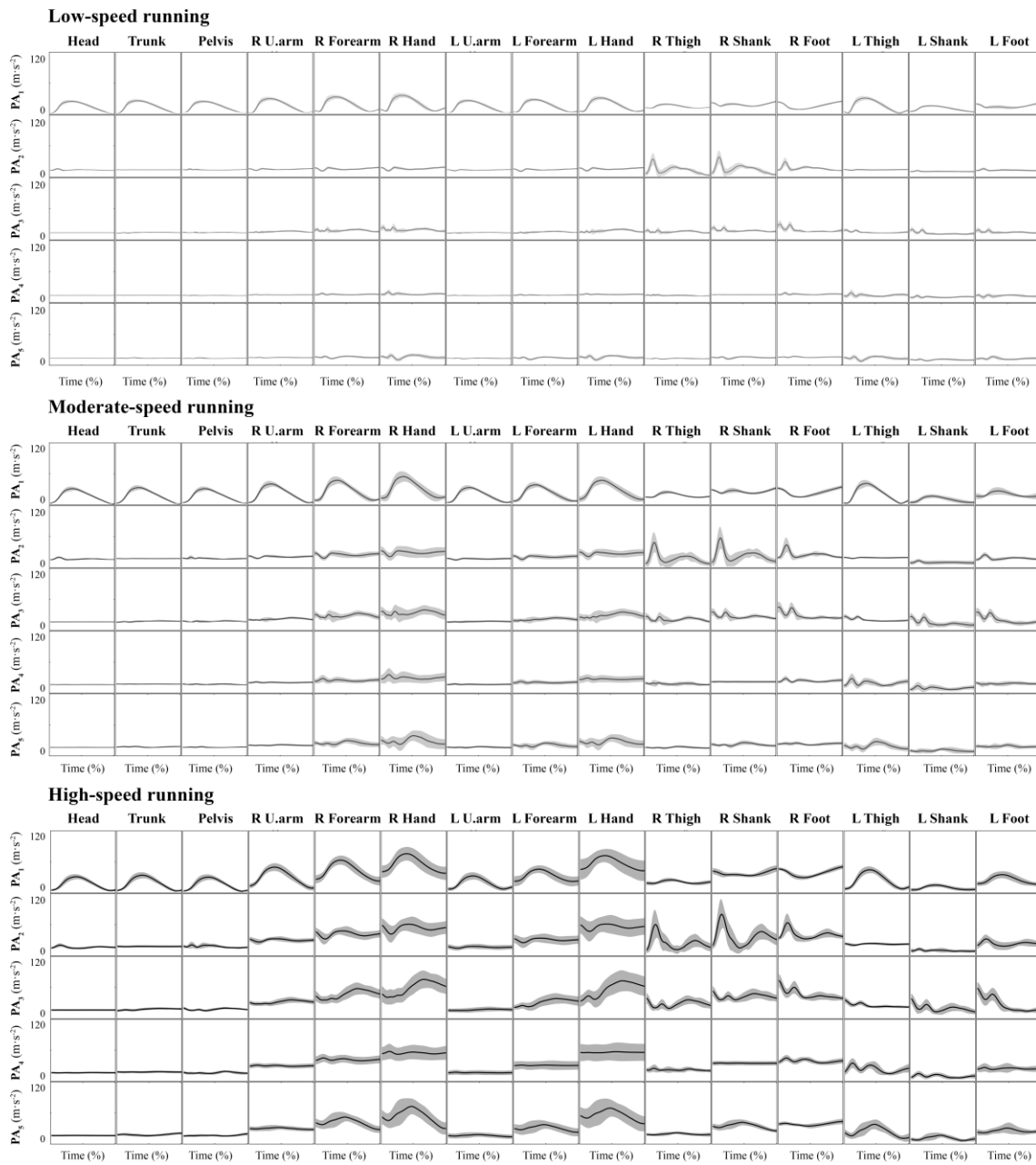


407 **Figure A.1** Principal accelerations (PAs) from the first five principal components (rows) for
 408 accelerations (blue), decelerations (red) and 90° cuts (green) during a right leg contact phase. PA
 409 profiles are mean \pm standard deviation (shaded) curves from 0-100% of stance, for all fifteen segments
 410 (columns).

411

412

413



414 **Figure A.2** Principal accelerations (PAs) from the first five principal components (rows) for running
415 at constant low (light grey), moderate (grey) and high speeds (black) during a right leg contact phase.

416 PA profiles are mean \pm standard deviation (shaded) curves from 0-100% of stance, for all fifteen
417 segments (columns).

418